Bio-catalytic hydrolysis of paper pulp using in- and ex-situ multi-physical approaches: Focus on semidilute conditions to progress towards concentrated suspensions

Tien Cuong Nguyen, Dominique Anne-Archard, Xavier Cameleyre, Eric Lombard, Kim Anh To, Luc Fillaudeau

BIO-CATALYTIC HYDROLYSIS OF PAPER PULP USING IN- AND EX-SITU MULTI-PHYSICAL APPROACHES: FOCUS ON SEMIDILUTE CONDITIONS TO PROGRESS TOWARDS CONCENTRATED SUSPENSIONS

Tien Cuong NGUYEN[a,b,d*], Dominique ANNE-ARCHARD[b,c], Xavier CAMELEYRE[a,b], Eric LOMBARD[a,b], Kim Anh TO[d] and Luc FILLAUDEAU[a,b]

[a] Laboratoire d'Ingénierie des Systèmes Biologiques et des Procédés (Université de Toulouse; INSA; INRA UMR792, CNRS UMR5504), Toulouse, France

[b] CNRS, Fédération de Recherche FERMAT (FR 3089), Toulouse, France

[c] Université de Toulouse, Institut de Mécanique des Fluides de Toulouse, Allée Camille Soula, F-31400 Toulouse, France

[d] School of Biotechnology and Food Technology, Hanoi University of Science and Technology, Hanoi, Vietnam

*__Corresponding author__: cuong.nguyentien1@hust.edu.vn

__Permanent address__: School of Biotechnology and Food Technology, Hanoi University of Science and Technology, 1 Dai Co Viet Road, Hanoi 100000, Viet Nam

__Telephone__: (+84) 989443105; __Fax__: (+84) 2438682470

Abstract

In order to make 2nd-generation biofuels more competitive, high solid-matter content has to be reached. To progress towards this target, the mechanism for destructuring lignocellulose fibres in semidilute conditions has to be well understood, as this configuration shows the basic mechanism which limits transfers and efficiency. This study aims to delve deeply into the biophysical and transfer limitations occurring during enzymatic hydrolysis. A specific experimental set-up associating in-situ and ex-situ physical (rheometry, chord length analysis) and biochemical analysis was used to expand the knowledge of hydrolysis of extruded softwood paper pulp over 24 h under different substrate concentrations (1% to 3%) and enzyme doses (Accellerase 1500, 5 and 25 FPU/g cellulose). Non-Newtonian behaviour associated with pronounced yield stress stand as the major factors limiting process efficiency. A critical time was deduced from viscosity evolution, and the existence of a unique, dimensionless viscosity-time curve was established, suggesting similar mechanisms for fibre degradation. In addition, chord length distribution allowed for the description of population evolution and was discussed in the light of in-situ viscosity and hydrolysis yield. Physical (viscosity, particle size) and biochemical (substrate) kinetics were modelled (second-order) and coefficients identified. A chronology of the encountered phenomenological limitations demonstrates the necessity of optimising bioprocesses by considering physical parameters. A reference feed rate is proposed in order to reach high solid loading under fed-batch strategy.

Keywords: biorefinery; enzymatic hydrolysis; kinetics modelling; paper pulp; rheometry; yield stress.

Nomenclature

C	Torque (mixing system)	(N.m)
Cm	Mass concentration	($gdm.L^{-1}$)
Cellu	Cellulose content	(%)
DM	Dry matter content	(% $g.L^{-1}$)
DP	Degree of polymerisation	(/)
E/S	Enzyme/substrate ratio	($mL.g^{-1}$)
[Glc]	Glucose concentration	($g.L^{-1}$)
G'	Elastic modulus	(Pa)
G"	Viscous modulus	(Pa)
Kp	Power constant	(/)
Ks	Metzner-Otto constant	(/)
k_μ	Rheological kinetic coefficient	($Pa^{-1}.s^{-2}$)
k_{lc}	Granulometric kinetic coefficient	($\mu m^{-1}.s^{-1}$)
k_S	Biochemical kinetic coefficient	($(gdm/L)^{-1}.s^{-1}$)
lc	Chord length	µm
lc_m	Mean chord length	µm
m_s	Quantity of substrate	(g humid matter)
N	Rotation speed	(revolutions per second)
Np	Power number	(/)
P	Power consumption	(W)
Re	Reynolds number	(/)
R^2	Correlation coefficient	(/)
V_w	Water volume	(L)
$\dot{\gamma}$	Shear rate	(s^{-1})
ρ	Density	($kg.m^{-3}$)

ρ_s	Substrate density	($kg.m^{-3}$)
μ	Viscosity	(Pa.s)
μ_0	Initial viscosity	(Pa.s)
μ_∞	Final viscosity	(Pa.s)
μ^*	Dimensionless viscosity	(/)
τ	Shear stress	(Pa)
τ_0	Yield stress	(Pa)

45

1 Introduction

The latest global agreement, the Paris agreement, was established in 2015 to reduce the scale of the fossil-fuel-based economy. Greater use of renewable resources with low carbon footprints is being advocated to substitute the usage of fossil fuels and to achieve the goal of a decarbonised economy. Biofuel stands as one potential alternative, and is being scrutinised in many countries [1]. This development is not only justified by economic reasons, but also by societal demand and environmental constraints that necessitate the move towards renewable energies. Cellulosic biomass provides a low-cost, renewable, and abundant resource that has the potential to support large-scale production of fuels and chemicals via biotechnological routes [2]. Among the major users of lignocellulose resources generated through forestry and agricultural practice, the pulp and paper industry holds a strategic position. Currently, the promotion of biorefineries producing multiple products, including higher-value chemicals as well as fuels and power, is a major objective of numerous consolidated programs in the world. In order to achieve economic viability, the biorefinement of lignocellulosic resources must be operated at very high feedstock dry matter content. This strict prerequisite imposes a considerable constraint, particularly on the physicochemical and biocatalytic steps, which, overall, aim to produce high-quality, fermentable sugar syrups. Moreover, industrial criteria regarding maximum reactor volumes, energy and water consumption, and wastewater management must also be respected. The pulp and paper industry is able to provide a tried and tested industrial model for processing lignocellulose biomass into pre-treated cellulose pulps. The pulp product of this industry is appropriate for modern biorefining because it displays low lignin content, is free of inhibitory compounds that can perturb fermentations, and is devoid of microbial contaminants [3]. The process of biofuel production can thus be coupled with the pulp and paper industry. Two main advantages are highlighted here. The first is the perfect control of paper pulp quality due

72 to the efficiency of woody substrate pre-treatment and to the elimination of the lignin
73 fraction in the initial biomass. The second is that the pulp and paper industry produces
74 energy by valorising residues and co-products, thus reducing final biofuel costs [4].
75 In order to produce 2nd-generation biofuels, pre-treated paper pulp would be hydrolysed
76 and then fermented to convert the simple sugars (hexoses and also pentoses) into
77 molecules of interest. Conventionally, this process involves two separate steps:
78 hydrolysis and fermentation (SHF). In addition, it can also use simultaneous
79 saccharification and fermentation processes or, more recently, consolidated
80 bioprocessing, which integrates enzyme production, saccharification, and fermentation
81 into a single process. In the SHF process, cellulose is enzymatically hydrolysed by
82 cellulases during the first step to form simple sugars (e.g. glucose), which are consumed
83 in the second step by *Saccharomyces*, *Zymomonas,* or other microorganisms to obtain
84 the desired product [5-7]. The main advantage of SHF is the ability to carry out each
85 step in its optimum conditions: temperature, pH, etc.
86 The key steps are always the pre-treatment techniques and the conversion into
87 fermentable sugars [8]. A better scientific understanding, and ultimately exact technical
88 control, of these critical biocatalytic reactions, which involve complex matrices at high
89 solid content, currently pose a major challenge that must be overcome to facilitate the
90 intensification of biorefining operations. Among the main parameters to be studied, the
91 rheological behaviour of the hydrolysis suspension and the fibre particle size stand out
92 as major determinants of process efficiency, and are responsible for the choice of
93 equipment to be used and the strategies to be applied [9]. Nevertheless, only a limited
94 number of studies cover the rheological behaviour of lignocellulose matrices in highly
95 concentrated suspensions during biocatalytic degradation [10].
96 The purpose of this study was to investigate the destructuring of fibre during enzyme
97 attack under a multi-scale approach using different analytical techniques. Semidilute
98 conditions were chosen, as they introduce the complexity of particle-particle

interactions, which are strongly involved in the transfer limitations observed in high dry matter content, without inhibiting the bioreactions. **Figure 1** illustrates the three blocks corresponding to the three levels of observation: macro-scale with viscometry and rheometry, micro-scale with chord length distribution (CLD) and molecular scale with biochemistry (chemical analyses of soluble fraction and solid fraction). This three-membered framework permits the analysis and comparison of in- and ex-situ methods (excluding biochemical analysis). Experiments were conducted using three substrate concentrations in a semidilute regime and two enzyme concentrations to explore the impact of substrate properties and enzyme ratio on fibre destructuring kinetics (bioconversion rate). Then, phenomenological models can be established and considered as a whole to provide a full overview of the mechanism. In this regard, the phenomenological models should fulfill certain criteria, such as reliability, simplicity, and congruity with the experimental information. It is hoped that a global result from these three sub-blocks will provide a "knowledge block" to explain certain scientific limitations and lead to the implementation and intensification of considered bioprocesses.

2 Materials and Methods

2.1 Experimental set-up

An experimental set-up was specifically developed which consisted of a bioreactor and a home-designed impeller system associated with several in-situ sensors (temperature, pH, rotation speed, torque, FBRM sensor). The bioreactor was a homemade glass tank (diameter: 130 mm, H_{max}: 244 mm, V: 2.0 L) with a water jacket for thermal regulation. A specific agitator included a double impeller to minimise the difficulty in substrate mixing and ensure suspension homogeneity (**Figure 2**). The first impeller consisted of three inclined blades (diameter: 73.5 mm, angle: 45°, h = 38 mm) located 75 mm above the bottom to ensure mixing. The second mixer, which had 2 large blades (diameter:

120 mm, h = 22 mm), was set close to the bottom to avoid substrate decantation. The impeller shaft was connected to a viscometer working at a set speed (Viscotester Haake VT550, Thermo Fisher Scientific). This allowed for on-line torque measurements. The rotational speed ranged between 0.5 and 800 rpm, and torque ranged between 0.1 and 30 mN.m (< 400 rpm) and 20 mN.m (> 400 rpm) (accuracy ±0.5%). Temperature was controlled by circulation (Haake DC30 cryostat, -50 to 200 °C ±0.01, Thermo Scientific) through the water jacket. Suspension pH was monitored by a pH meter (Mettler Toledo Seveneasy S20, 0-14±0.01, -5 to 105 °C) and the pH adjusted with 0.5 N NaOH or 0.5 N H_2SO_4. The viscometer and the cryostat were controlled by HaakeRheoWin Job Manager software (Thermo Fisher Scientific) which also ensured data recording (temperature, torque, mixing rate). A focused beam reflectance sensor (FBRM-G400-Mettler Toledo, range of 0.1 to 1000 µm) was located in the reactor in order to measure the distribution of particle chords.

2.2 Substrates and enzyme

Paper pulp from coniferous wood (Softwood, obtained via the Kraft process, with pulp extracted before bleaching, Tembec Co., Saint-Gaudens, France, type FPP27) after extrusion (Extruder Eurolab 16, 400 mm failure, extrusion line: 25 L/D 18/25 conveying, 7/25 shear stress) was selected for study. The humidity of this substrate was 72%. Per unit dry weight it contained 82% cellulose, 8% hemicellulose, 2% lignin, the remainder being ashes (3%) and extractive fractions (2-4%) whose composition has not been determined. The substrate density is 1034±9 ($kg.m^{-3}$) and the mean volume dimeter of particles is 497±77 (µm). This pulp is favourable for enzymatic hydrolysis because of its low lignin content (2%). It also contains a low proportion of hemicellulose (xylan, mannan, etc.).

An enzyme cocktail (ACCELLERASE® 1500 Genencor, USA, ref. 3015155108) containing exoglucanases, endoglucanases (2200 to 2800 CMC U/g), hemicellulases

and β-glucosidases (525 to 775 pNPG U/g) was used. Its optimal temperature and pH were 50 °C (range 50 to 65 °C) and 4.8 (range 4 to 5), respectively. An ACCELLERASE® 1500 dosage rate of 0.1 to 0.5 mL per gram of cellulose or roughly 0.05 to 0.25 mL per gram of biomass (depending on the biomass composition) was recommended by the suppliers. Inactivation may occur at temperatures higher than 70 °C and for pH < 4 or pH > 7. Enzyme activities were characterised in the range of 50 to 60 FPU/mL as reported [11, 12].

2.3 Physical analysis

Lignocellulose suspensions demonstrate complex rheological behaviour, and there is no standard method for studying their flow behaviour. To characterise their rheological properties as finely as possible, two measurement strategies were combined: (i) ex-situ rheometry (oscillation mode), which provided yield stress and elasticity information, and (ii) in-situ viscometry, which followed suspension viscosity in real time during enzyme attack. Particle size was analysed by in-situ chord length measurement (FBRM).

2.3.1 Ex-situ rheometry

Classic rheometry based on continuous permanent shear rate appears irrelevant for lignocellulosic substrates because of the rapid aggregation of fibres [10]. Thus, oscillatory measurements (including strain sweeps and frequency sweeps) were performed. These measurements offer several advantages: firstly, they prevent fibre aggregation caused by constant unidirectional shear flow; secondly, they provide additional information on the rheological behaviour of the suspensions (yield stress in this case). The storage modulus G' and the loss modulus G'' were measured using a Mars III rheometer (Thermo Scientific). Dynamic measurements were performed with serrated plates (60 mm, roughness 400 µm, gap size: 1.5 mm) on samples taken during hydrolysis. First, an oscillatory shear flow was set up with increasing shear stress

177 amplitude from 0.1 to 20 Pa and at a fixed frequency (1 Hz). This first measurement
178 was used to determine the linear domain. Then a scan was carried out in the linear
179 domain for frequencies from 0.5 Hz to 20 Hz and fixed shear stress amplitude. The
180 analysis was performed at 20 °C. Several methods can be used for yield stress
181 determination. It can be interpreted as the stress amplitude at which the elastic modulus
182 G' becomes smaller than the shear modulus G", or as the stress amplitude at which the
183 loss modulus G" reaches a maximum. It can also be identified as the maximum elastic
184 stress verifying a linear relation $\tau = G'.\gamma$ where γ is the strain amplitude [13, 14].
185 Especially for lignocellulose substrates, which cannot stand long measurement times, it
186 was defined as the first departure from the linear viscoelastic region [9, 15]. In the
187 present study, a 20% reduction in G' was chosen.

188 **2.3.2 In-situ rheometry**

189 Ex-situ measurement was limited by the number of samples and the substrate properties,
190 predominately decantation and flocculation of material. To overcome these difficulties,
191 in-situ viscometry was conducted throughout hydrolysis. It was based on the
192 determination of power consumption (or power number
193 $Np = \frac{P}{d^5 \cdot \rho \cdot N^3}; P = 2\pi \cdot N \cdot C$) versus the Reynolds number ($\mathrm{Re} = \frac{\rho \cdot N \cdot d^2}{\mu}$) during
194 suspension mixing (see [16] for details). The viscosity was calculated from the power
195 consumption curve of the mixing system under consideration using a semi-empirical
196 model including laminar and transition regions for the reference curve with a one-to-one
197 relationship between Np and Re:

198 $$Np = \left(\left(\frac{Kp}{\mathrm{Re}} \right)^q + N_{p0}^q \right)^{1/q} with: N_{p0} = 0.128; q = 0.782 \quad (Eq.\ 1)$$

199 The Kp constant for the mixing system was 97.9, while the Metzner-Otto constant used
200 to estimate an equivalent shear rate was Ks = 32. All the geometric constants were

201 determined from measurements using Newtonian (water, Marcol oil, and glycerol) and
202 non-Newtonian fluids (xanthan-sucrose solutions). Once the experimental set-up was
203 characterised by its power consumption curve Np(Re) and its Ks value, in-situ
204 viscometry of the suspension was performed before the addition of enzymes and then
205 throughout the biocatalytic reaction.

206 **2.3.3 In-situ particle size analysis**

207 Focus beam reflectance measurement (FBRM) enabled in-situ quantification and
208 characterisation of chord length distribution (CLD). The FBRM sensor (FBRM G400,
209 Mettler-Toledo, range: 0.1 to 1000 μm) was set up in the bioreactor to detect and
210 monitor the changes of particle dimensions during enzymatic hydrolysis in real time.
211 FBRM measurement is a laser-based technique. A solid-state laser light source (λ = 795
212 nm) provides a continuous beam of monochromatic light that is sent down the FBRM
213 probe. A precision motor—pneumatic or electric—is used to rotate the precision optics
214 at a constant speed. The scan speed is fixed at 2 $m.s^{-1}$. As the scanning-focused beam
215 sweeps across the face of the probe window, individual particles or particle structures
216 (agglomerated or floc) backscatter the laser light towards the probe. Particles and
217 droplets closest to the probe window are located in the scanning focused spot and
218 backscatter distinct pulses of reflected light, which are detected by the probe and
219 translated into chord lengths based on the simple calculation of the scan speed (velocity)
220 multiplied by the pulse width (time). A chord length is simply defined as the straight-
221 line distance from one edge of a particle or particle structure to another edge. Typically,
222 thousands of individual chord lengths are measured each second to produce the chord
223 length distribution, which is the fundamental measurement provided by FBRM.

2.4 Biochemical analysis

2.4.1 Dry matter content

The water content of substrates and hydrolysed suspensions was determined by drying at low temperature and pressure. Volumes of samples (≈1 mL) were put in Eppendorf tubes (known mass, m_{epp}). These Eppendorfs (m_{ini}) were then placed in an oven at 60 °C, 200 mbar for 5 days, and afterwards, weighed (m_{fin}). Water content (W) and dry matter content (DM) were calculated using **Eq. 2** (accuracy ±0.5%):

$$W(\%) = \frac{m_{ini} - m_{fin}}{m_{ini} - m_{epp}} \cdot 100; DM(\%) = 100 - W \quad \textit{(Eq. 2)}$$

2.4.2 Monomers and oligomers

Samples were centrifuged at 13000 rpm for 5 min. Glucose and soluble cello-oligosaccharides, (i.e. with a degree of polymerization lower than 6) in the supernatants were quantified by an AMINEX HPX-87P carbohydrate analysis column (Bio-Rad Laboratories, Richmond, CA) using a high-performance liquid chromatography system (separations module: Waters Alliance 2690; refractometer detector: Waters 2414, Milford, MA). Conditions were optimised to detect and quantify the different cello-saccharides. Analysis was performed at 60 °C with deionised water and 0.1M $Pb(NO_2)_2$ as mobile-phase (ratio 80/20 v/v) at a flow rate of 0.5 mL/min for 30 min. Glucose and cello-oligosaccharide standards with a DP ranging from 2 to 5 were used (Sigma Chemical Co., St. Louis, MO).

2.5 Experimental strategy

Enzyme hydrolysis was carried out at 40 °C due to enzyme heat stability (activity reduction at high temperature), energy conservation, and taking into account the optimal conditions for the cell cultivation step. The pH of the medium was adjusted to 4.8. To prevent microbial contamination, 0.2 mL of a solution of chloramphenicol (5 $g.L^{-1}$) was

added. Enzymes were added when the suspension reached homogeneity (visual monitoring and stabilised torque, reached within 30 min). Hydrolysis was carried out over 24 h with a mixing rate of 100 rpm (corresponding approximately to a shear rate of 50 s^{-1}), reactor volume 1300 mL and using three substrate concentrations, 1% (10.1 and 9.7 gdm/L formally), 2% (only for in-situ viscometry analysis, 19.6 and 20.0 gdm/L formally) and 3% w/v (29.2 and 28.7 gdm/L formally), two enzyme/substrate ratios, 0.1 and 0.5 mL enzyme/g cellulose respectively (corresponding to 5 and 25 FPU/g cellulose). Suspensions were sampled with a 7 mm diameter flexible tube connected to a 50 mL syringe. Each sample was about 15 mL at 0 h, 15min, 1h, 2h, 3h, 5 h, 7h, 10 h and 24 h of hydrolysis time. The enzyme reaction was stopped by adding 0.1 mL 10 N NaOH. The total volume of samples removed was approximately 130 mL (< 10% of initial volume). Samples were analysed in terms of rheological, granulo-metric and biochemical properties during enzyme degradation.

3 Results and Discussions

3.1 Bioconversion rate

The production of monomers (C6, C5) and water-soluble oligosaccharides is crucial for the development of new intensified bioprocesses. First of all, the bioconversion rate was calculated from the glucose produced using **Eq. 3**.

$$Bioconversion\,(\%) = \frac{[Glc]_{measured}}{[Glc]_{theory}}$$

$$[Glc]_{theory} = \left(m_s \cdot \frac{DM}{100} \cdot \frac{Cellu}{100 \cdot 0.9} \right) \Big/ \left(V_w + \frac{m_s}{\rho_s} \right) \quad \textit{(Eq. 3)}$$

The theoretical conversion coefficient from cellulose to glucose is 1/0.9.

Under enzyme activity, the polymeric cellulose chain is broken down to produce monomers. Oligomers (DP > 2) were not detected for any of the experiments. Xylose was quantifiable only in the case of 3% w/v - 0.5mL enzyme/g cellulose.

As expected, the concentration of monomers (glucose, xylose) increases with hydrolysis time. For example, in the 3% w/v cases, the monomer concentration increased regularly during hydrolysis, so that enzyme loading had an impact on the quantity of the glucose released: 5.1 to 19.1 $g.L^{-1}$, which corresponds to 19 and 73% bioconversion for 0.1 and 0.5 mL/g cellulose respectively (**Table 1**). Few articles have examined the evolution of water-soluble cello-oligosaccharides. Sun and Cheng [17] analysed the hydrolysis of microcrystalline cellulose (10 $g.L^{-1}$) by cellulase produced by *Cellulomonas fimi*. They did not detect soluble oligomers with DP≥4, but the cellotriose concentration varied between 0.2 and 0.6 $g.L^{-1}$ depending on the enzyme used—endo-glucanase or cellobiohydrolase. Solubilisation reached 61% and 50% respectively for each enzyme separately. In contrast, the intermediates of cellulose hydrolysis were not found because the Accellerase 1500 cocktail contains all the types of activity required to rapidly degrade these intermediates during hydrolysis.

The bioconversion yields are comparable to data reported in the literature. For a 2% (w/w) suspension of oven-dried corncob, after 24 h hydrolysis the glucose conversion varied between 30 and 82% for 6 and 30 FPU/g [18]. With the hydrolysis of a pre-treated wheat straw suspension at 1% (w/v), a doubled bioconversion (from 45.9 to 87%) after 18 h with enzyme loading between 9.6 and 57.6 FPU/g was reported [19].

Changes in dry matter content were monitored by determining the water content in the sample at different hydrolysis times. This technique involves the error inherent to sampling heterogeneous suspensions. Beside this technique, the dry matter content was also determined from dissolved and undissolved substrate measurements. According to the hypothesis of the conservation of substrate mass before and after hydrolysis, the dry matter in suspension can be deduced from the initial quantity and the hydrolysed quantity (which released soluble components—monomers and cello-oligosaccharides). As previously reported, the water-soluble cello-oligosaccharides with DP > 2 were not

297 quantifiable, so only glucose, xylose, and cellobiose were used to calculate the quantity
298 of hydrolysed substrate. Mass balance was conserved around 95% (**Table 1**).

299 ## 3.2 Rheological behaviour during hydrolysis

300 ### 3.2.1 Viscosity and yield stress

301 In-situ viscometry showed that substrate suspensions were non-Newtonian shear-
302 thinning fluids. The viscosity of suspensions at 100 rpm (corresponding to an equivalent
303 shear rate of 50 s^{-1}) as a function of hydrolysis progress is illustrated in **Figure 3-A**. As
304 expected, slurry viscosity decreased during hydrolysis. Excluding the very beginning of
305 the reaction ($t < 0.2$ h), viscosity changed drastically at the beginning of hydrolysis.
306 This sharp reduction in viscosity was observed whatever the concentration or
307 enzyme/substrate ratio. For example, at 3% dm (w/v), 0.5 mL E/g cellulose, the
308 viscosity decreased from 68 to 3 mPa.s. This change in the physical appearance of the
309 slurry is associated with the biochemical changes and particle size changes occurring in
310 the fibres [20, 21]. The drop in viscosity is a combination of the decrease of solid
311 concentration (solubilisation) and of the fragmentation of cellulose fibres [22, 23].
312 Under the effects of enzymes, the cellulose chains are broken up to produce smaller
313 particles and non-dissolved cellulose is converted into soluble compounds such as
314 monomers and water-soluble oligomers. In addition, the viscosity drop is suggested to
315 be strongly connected with the degradation and decrease in water binding capacity of
316 the lignocellulose matrices during enzyme-based hydrolysis [24].
317 The initial viscosities of the 3% (w/v) suspensions were 14-fold higher than those of the
318 1% (w/v) suspension (~70 and ~5 mPa.s, respectively). The nonlinear dependence of
319 viscosity on the concentration is expected and can be explained by an increase in
320 particle interactions, less free water, and hydrogen bonding between cellulose chains.
321 As the solid concentration increases, the average distance between particles in the slurry
322 decreases, leading to enhanced contact between particles, especially if there is an

entanglement of amorphous fibres between particles [25]. The high increase in initial viscosity of between 1% (w/v) and 3% (w/v) signifies that the increase of substrate concentration becomes the major stress for enzymatic hydrolysis at high (and very high) dry matter content levels. That is why a special strategy to reach the condition of high substrate concentration is absolutely necessary. During hydrolysis, a significant drop in slurry viscosity is observed within the first 10 h of the hydrolysis reaction. These results are supported by the literature for a wide range of matrices, particle sizes, and enzyme/cellulose ratios [26-28], although a large heterogeneity of viscosity data is reported. This can be explained by different substrates, pre-treatments, morpho-granulometry and enzymes, and operating conditions.

The effect of enzyme concentration on viscosity is clearly demonstrated even for the lowest concentration in **Figure 3-A**. For the same substrate concentration, the higher the enzyme/g cellulose ratio (E/C), the faster the viscosities decrease. Within 5 h, the viscosity of a 3% (w/v) suspension was reduced by 85% for 0.5 mL E/g cellulose; whereas its reduction was limited to 30% for 0.1 mL E/g cellulose. This observation is in agreement with other authors [22, 26, 29]. Furthermore, two tendencies in viscosity evolution were found for suspensions containing 0.1 mL/g cellulose. Firstly, the suspension viscosity increased during the first hour consecutive to swelling and unbinding effects (clearly observed for 2% w/v and 3% w/v, not significant for 1% w/v); after that, the viscosity decreased because of depolymerisation by the enzymes.

Shear stress sweep and frequency sweep experiments were performed in oscillation mode (see §2.3.1). The frequency sweep revealed that the elastic modulus G' and the viscous modulus G'' do not depend on frequency (**Figure 3-B**). In addition, G' is always greater than G'', with a ratio G'/G'' which can be identified in Figure 3-B. This is characteristic of viscoplastic behaviour, and shear stress sweeps were then used to evaluate yield stress. All suspensions showed viscoplastic shear-thinning behaviour both initially and throughout hydrolysis. Shear-thinning has already been mentioned by

other authors [9, 27, 29]. Before the introduction of enzyme, the rheological behaviour for small deformations is mainly elastic, with a high value of G' and a ratio G'/G'' close to 5. For a 3% (w/v) suspension at t = 0 h and in the linear domain, G' and G" reached about 1000 and 200 Pa. This is supported by the literature for different matrices. For corn stover, at 12% dm, G' and G" were reported as 2000 and 300 Pa [15]; for acid pre-treated softwood, these values were 100 and 50 Pa respectively [9]. When increasing the shear stress, all the samples exhibited two zones: a first where G' and G" did not depend on shear stress (linear domain) and a second where both moduli decreased. In this second zone, G' deviated sharply from a stable curve and crossed (or tended to cross) G". During hydrolysis, a regular decrease in both moduli was observed. For example, in the 3%-0.5 case, a 1000-fold reduction was observed for both G' and G" after 24 h of enzyme attack. Moreover, the elastic character is noticeably preserved. One also notes that the higher the enzyme activity, the faster the decrease in elasticity (in agreement with the viscosity results above). This discussion highlights, yet again, the strong impact of enzyme concentration on how rheological behaviour varies during hydrolysis.

As viscometric yield stress measurements were not possible for these suspensions, this yield stress τ_0 was deduced from the elastic modulus (G') (see **Figure 3-B**). Yield stress can be regarded as the stress required to initiate flow. Yield stress values between 1 and 20 Pa were determined at 1% and 3% dm (w/v) before hydrolysis. With an increase in substrate concentration from 1% to 3% dm (w/v), yield stress increased 20-fold (**Figure 4**). This confirmed the critical substrate concentration (≈3% dm (w/v) determined by in-situ measurements) beyond which the viscosity increased exponentially [16]. The results presented were slightly higher than those obtained from pre-treated softwood: 0-28 Pa for 4-12% substrate concentration [9] and from pre-treated corn stover: 0.26-22.9 Pa for 5-17% dm [30]. This difference could be due to the nature and the physical characteristics of the matrices and to the method used to determine yield stress.

During hydrolysis, yield stress decreased sharply as enzyme attack progressed (**Figure. 4**). This can be explained by the drop in solid content in suspension and by a reduction in fibre-fibre interactions due to hydrolysis progress. The decrease of yield stress was greater for experiments with higher enzyme concentrations. The final yield stress (at 24 h hydrolysis) of 3%-0.1 was 10 times higher than that of 3%-0.5. This observation is directly correlated to the impact of enzyme activities on fibre degradation. In addition, the yield stress of the hydrolysed samples (3%-0.5 at 24 h, DM = 1.14%) exhibited lower values for similar DM content compared to the original material (yield stress at 0 h of 1% - 0.5, DM = 0.97%). This can be explained by the modification of fibre structure, diameter, and shape. Decreasing yield stress during enzyme hydrolysis was previously reported for corn stover [21] and pre-treated softwood [9]. These two studies also reported a lower yield stress value for hydrolysed slurries when compared to non-hydrolysed slurries at the same solid content.

Figure 4 shows the dependence of yield stress during hydrolysis presented in terms of dry matter content. Taking the criterion that the fluid behaves as a pourable liquid at a yield stress below 1 Pa (the values of 1% are negligible), interestingly, results for 3% show that the two yield stress curves collapse onto a single curve when plotted against dry matter content. It decreased exponentially with the decrease in dry matter content during hydrolysis. Yield stress becomes negligible when solid matter < 2%. This has real significance for the choice of substrate flow rate for the cumulative feed strategy or if the slurry has to be pumped into another bioreactor.

3.2.2 Uniqueness of viscosity-time curve

In order to explore the change in viscosity during enzyme hydrolysis and to compare its kinetics between different experimental conditions, a critical time is estimated through a normalised viscosity defined as follows:

401 $$\mu^* = \frac{\mu_t - \mu_{fin}}{\mu_0 - \mu_{fin}} \textit{(Eq. 4)}$$

402 μ^* is a dimensionless viscosity; and μ_0, μ_t, μ_{fin} are the viscosities at t = 0 h, t_i and the
403 final viscosity (the viscosity of a suspension containing the whole dry matter as soluble
404 fractions – hypothesizing total conversion).
405 μ^* describes the reduction of viscosity during enzyme hydrolysis. It starts from 1 (t = 0
406 h) and tends to 0 (t = 24 h). From this quantity, a critical time noted $t(\mu^* = x)$ can be
407 defined as the time at which the viscosity was x% of the initial suspension viscosity.
408 The relationship between these critical times $t(\mu^* = x)$ and dimensionless viscosity, μ^*
409 only depends on the enzyme concentration used regardless of the substrate
410 concentration. These critical times decreased exponentially with the dimensionless
411 viscosity. The ratio of these critical times between both conditions was around 4-fold.
412 Thus the hydrolysis time, t, can be normalised using a selected critical time $t(\mu^* = x_0)$
413 **(Eq. 5)**:

414 $$t^* = \frac{t}{t(\mu^* = x_0)} \textit{ (Eq. 5)}$$

415 The dimensionless time-viscosity curves are plotted in **Figure 5** (μ^* = 0.25).
416 Interestingly, a single curve is exhibited for $t^* > 0.05$, i.e. when the possible swelling
417 and unbinding effects can be neglected. This uniqueness of dimensionless time-
418 viscosity curves was observed whatever the hydrolysis conditions in the studied cases
419 (substrate concentrations, enzyme ratio). These results suggest that during the period
420 and for a 75% reduction of initial viscosity, a similar degradation mechanism could be
421 assumed in semidilute regime (≤3% dm w/v), although rheological behaviour strongly
422 differs between 1% and 3% w/v suspensions.
423 The uniqueness of viscosity-time curves at macroscopic observation suggests a similar
424 mechanism of fibre degradation. Considering these in-situ and ex-situ rheological

425 results, macro scales will be explored with chord length distribution analysis, and then
426 kinetics will be modelled.

427 **3.3 Particle size evolution**

428 The time evolution of the mean chord length and chord number for the four different
429 conditions is shown in **Figure 6**. Considering chord length distribution (CLD) for the
430 initial suspension, we define four classes (I: < 60 µm, II: 60 to 90, III: 90 to 160 µm, IV:
431 160 to 600 µm) which correspond to 25% of this population. **Figure 7** illustrates the
432 evolution of each class during hydrolysis for the case 1% w/w - 0.5 mL enzymes/g
433 cellulose.
434 A sharp decrease in mean chord length from 120 to 60 µm (**Figure 6**) is observed:
435 within two hours for E/S = 0.5 mL/g and six hours for 0.1 mL/g. Considering chord
436 number, initial values are almost proportional to concentration and during hydrolysis,
437 two successive trends are observed. During the first step, the total chord number
438 increased for all experiments, although the durations of this step differed strongly:
439 around 8 to 10 hours for E/S = 0.1 mL/g, and 1 to 3 hours for E/S = 0.5 mL/g.
440 Meantime, the relative increase of chord number is lower for the largest E/S ratio.
441 Considering now **Figure 7**, coarse population (class IV) decreased regularly while the
442 finest population (Class I) increased.
443 The initial augmentation of chord number can be explained by the fragmentation of
444 cellulose fibres. Coarse particles are attacked and divided into several fine particles.
445 Beyond that, enzyme activity occurs and the finest particles are converted into dissolved
446 compounds, generating a reduction in chord number. As demonstrated in **Figure 6**, the
447 fragmentation mechanisms appear to be the dominant effect in the strong viscosity
448 reduction observed during the first 5 h, while solubilisation increased to 31%. In
449 contrast, after 5 h, fragmentation is negligible (class IV almost constant) while

450 solubilisation increased to 76% (at 24 h). Correlatively, the viscosity evolution was
451 limited and the finest populations still increased from 38% to 50%.

452 **3.4 Modelling kinetics at macro-, micro-, and biochemical scales**

453 Hydrolysis induces a reduction in particle size, dry matter content, and viscosity, which
454 promotes mixing and fibre accessibility. The kinetics of viscosity (macro), chord length
455 (micro) and substrate and product concentrations (biochemical) stand as key indicators
456 for understanding and controlling bioprocess performance. The kinetics of biochemical
457 enzymatic reactions have been extensively reported in the literature [31], contrary to
458 physical parameters such as viscosity and granulometry. A lot of enzyme reactions (e.g.
459 hydrolysis, oxidation, and reduction or cofactor mechanisms) are second- or higher
460 order reversible reactions. Many are limited by diffusion and physical accessibility.
461 Adsorption (reaction) in high molecular weight structures (for example, proteins,
462 polynucleotides, polysaccharides, or heterogeneous protein-phospholipid, protein-
463 nucleotide, and protein-polysaccharide structures) is more complex. Among the
464 numerous models reported in the literature, one of the best known is the Michealis-
465 Menten equation [32] but a first-order model was also reported by Chrastil [33].
466 The time evolution of viscosity μ, mean chord length lc_m, and residual substrate
467 concentration in dry matter S (%) are modelled by the general equation **Eq. 6**:

468 $$-\frac{dX}{dt} = k \cdot X^{\alpha} \quad (Eq.\ 6)$$

469 where X is the variable being modelled (μ, lc_m and S); k is the kinetic constant, and α
470 the model/reaction order (/). As boundary conditions, X varies from X_0 to X_∞,
471 corresponding to initial and final values respectively.
472 A second-order model accurately describes the time dependence of the physico-
473 chemical parameters—viscosity, chord length, and dry matter content. For the lowest
474 enzyme ratio, an increase of the mean chord length was observed during the first hours.

475 In these cases, the proposed model was restricted to the time interval corresponding to
476 the maximal value of lc_m until the end of hydrolysis (experiments with 0.1 mL
477 enzyme/g cellulose). This lc_m increase step could be explained by fibre swelling and
478 unwinding due to limited enzyme activity. To sum up, the most suitable kinetic models
479 are second order and written as **Eq. 7 to 9**:

480 $$\mu = \frac{\mu_0 - \mu_\infty}{(\mu_0 - \mu_\infty).k_\mu.t+1} + \mu_\infty \text{ (Eq. 7)}$$

481 $$lc_m = \frac{lc_{m0} - lc_{m\infty}}{(lc_{m0} - lc_{m\infty}).k_{lc}.t+1} + lc_{m\infty} \text{ (Eq. 8)}$$

482 $$S = \frac{S_0 - S_\infty}{(S_0 - S_\infty).k_S.t+1} + S_\infty \text{ (Eq. 9)}$$

483 The model was adjusted via the least squares method for each of the physico-
484 biochemical parameters. The coefficients and the correlation coefficients are presented
485 in **Table 2**. The correlation coefficients indicated the fine agreement between the
486 models and experimental data. The enzyme cocktail (Accellerase 1500) contained only
487 cellulases and hemicellulases, so the lignin fraction can be considered as contributing to
488 the non-hydrolysable fraction S_∞. For our substrate, lignin represents less than 2%, and
489 thus can be neglected. The final viscosity μ_∞ corresponds to the viscosity of a
490 suspension containing all soluble fractions (total conversion). In the present case, this
491 value would be close to the supernatant viscosity (0.7 mPa.s) and μ_∞ is negligible
492 compared to the initial suspension viscosity. In ideal conditions, the solid fractions
493 should be converted into soluble fractions and the ultimate chord length $lc_{m\infty}$ would then
494 be null. However, experimentally, there is always some part that remains non-
495 hydrolysable substrate, so $lc_{m\infty}$ cannot be neglected compared to lc_{m0}, and is assumed
496 equal to lc_{m24h}.
497 Effects of enzyme and substrate concentrations are clearly observed for all constants.
498 With k_S, the increase of the E/S ratio from 0.1 to 0.5 mL/g cellulose led to a 7- to 9-fold

499 increase. When the initial substrate concentration increased from 1 to 3% w/v, a
500 reduction of 2-3 times was observed. The same tendency was found with k_{μ}, which
501 demonstrated the strong impact of enzyme and substrate concentrations on the variation
502 of suspension viscosity during hydrolysis. Similar impacts were observed for enzyme
503 concentration and substrate concentration: 8-fold and 4-fold respectively. The final
504 value of the mean chord length, $lc_{m\infty}$, seemed identical in magnitude; however, the
505 impact of enzyme ratio can be clearly distinguished by the absolute values of k_{lc}. An
506 increase of 3.5-5.5 -fold of k_{lc} was observed when the enzyme concentration passed
507 from 0.1 to 0.5 mL/g cellulose.
508 Using equations 7 to 9, **Figure 8** illustrates the successive phenomenological limitations
509 observed during hydrolysis. Rheological behaviour appears to be the primary limiting
510 factor. Transfer limitation due to high viscosity and yield stress is, however, temporary
511 (during the first 5 h) but constitutes an important phenomenon. Viscosity collapse and
512 particle fragmentation are concomitant. Beyond this, the limited reduction in size
513 indicates a threshold for biocatalytic reaction. This could be due to recalcitrant fractions
514 or inefficient enzyme activities. It is therefore necessary to study the physical and
515 biochemical structures of this recalcitrant fraction in order to identify how it could be
516 degraded.
517 The major challenge in 2nd-generation biofuels is to reduce costs so as to compete with
518 1st-generation ones. Therefore, processing at high solid content is mandatory. However,
519 the rheological behaviour of the hydrolysis suspension stands out as the first and major
520 determinant of process efficiency, and has to be considered a key criterion in proposing
521 a rational strategy for reaching high dry matter content.
522 To increase transfers and bioreaction efficiency, a strategy can be built from the
523 identified parameters in a semidilute regime: the critical substrate concentration C*
524 (meaning a drastic increase of initial suspension viscosity beyond C*) and a targeted

hydrolysis time, t($\mu^* = x_0$) (corresponding to a chosen relative reduction of initial viscosity), can be used to define a reference feed rate Qc (**Eq. 10**):

$$Q_c = \frac{C^*.V}{t(\mu^*=x_0)} \ (g.h^{-1}) \quad \textit{(Eq. 10)}$$

A cumulative feeding strategy can be defined, based on Qc, which would allow working in a favourable regime so as to reach high hydrolysis yield by avoiding instantaneous high substrate concentrations.

4 Conclusion

This study aimed to delve deeply into the biophysical and transfer limitations occurring during enzymatic hydrolysis in the cellulosic biofuels context. Considering paper pulp substrates, semidilute conditions were chosen, as they introduce the complexity of particle-particle interactions, which are strongly involved in transfer limitations, without inhibiting the bioreaction. Biochemical and physical phenomena were explored through a specific experimental set-up associating in-situ and ex-situ analyses.

Non-Newtonian behaviour associated with non-negligible yield stress stand as the major factors limiting process efficiency and progress towards high solid loading. The uniqueness of dimensionless time-viscosity curves was observed whatever the operating conditions, and suggests a similar mechanism for fibre degradation. The evolution of biophysical parameters during hydrolysis was observed as the results of a combination of fibre fragmentation, which dominated during the first step, and solid solubilisation. Kinetics modelling enabled demonstration of the successive phenomenological limitations and their magnitude. All these elements lead to the proposal of a reference feed rate which would be used in a cumulative feeding strategy for reaching high solid loading and balancing energy consumption and process efficiency.

5 Acknowledgements

This work was realised within the ProBio3 project ANR-11-BTBR-0003, selected in the Investissements d'Avenir Programme, with financial support from the French government, managed by the National Research Agency. The authors are grateful to the "Programme de Bourses d'Excellence 2011" of the French Embassy in Vietnam.

References

[1] K.-H. Chang, K.-R. Lou, C.-H. Ko, Potential of bioenergy production from biomass wastes of rice paddies and forest sectors in Taiwan, Journal of Cleaner Production 206 (2019) 460-476.

[2] W.R. Gibbons, S.R. Hughes, Integrated biorefineries with engineered microbes and high-value co-products for profitable biofuels production, In Vitro Cellular & Developmental Biology - Plant 45(3) (2009) 218-228.

[3] P. Vallette, C. De Choudens, Le bois, la pêtes, le papier, Centre Technique de l'Industrie des Papiers, Cartons et Celluloses, 1987.

[4] M. Moshkelani, M. Marinova, M. Perrier, J. Paris, The forest biorefinery and its implementation in the pulp and paper industry: Energy overview, Applied Thermal Engineering 50(2) (2013) 1427-1436.

[5] Z.L. Fan, C. South, K. Lyford, J. Munsie, P. van Walsum, L.R. Lynd, Conversion of paper sludge to ethanol in a semicontinuous solids-fed reactor, Bioprocess. Biosyst. Eng. 26(2) (2003) 93-101.

[6] A. Herrera, S.J. Téllez-Luis, J.A. Ramírez, M. Vázquez, Production of Xylose from Sorghum Straw Using Hydrochloric Acid, Journal of Cereal Science 37(3) (2003) 267-274.

[7] X. Zhao, K. Cheng, D. Liu, Organosolv pretreatment of lignocellulosic biomass for enzymatic hydrolysis, Appl Microbiol Biotechnol 82(5) (2009) 815-827.

[8] T. Eggeman, R.T. Elander, Process and economic analysis of pretreatment technologies, Bioresource Technology 96(18) (2005) 2019-2025.

[9] M. Wiman, B. Palmqvist, E. Tornberg, G. Liden, Rheological characterization of dilute acid pretreated softwood, Biotechnol Bioeng 108 (2011) 1031 - 1041.

[10] T.C. Nguyen, D. Anne-Archard, L. Fillaudeau, Rheology of Lignocellulose Suspensions and Impact of Hydrolysis: A Review, in: R. Krull, T. Bley (Eds.), Filaments in Bioprocesses, Springer International Publishing 2015, pp. 325-357.

[11] P. Alvira, M.J. Negro, M. Ballesteros, Effect of endoxylanase and alpha-L-arabinofuranosidase supplementation on the enzymatic hydrolysis of steam exploded wheat straw, Bioresource Technology 102(6) (2011) 4552-4558.

[12] S.P. Govumoni, S. Koti, S.Y. Kothagouni, V. S, V.R. Linga, Evaluation of pretreatment methods for enzymatic saccharification of wheat straw for bioethanol production, Carbohydrate Polymers 91(2) (2013) 646-650.

[13] R. Damani, R.L. Powell, N. Hagen, Viscoelastic characterization of medium consistency pulp suspensions, Canadian Journal of Chemical Engineering 71(5) (1993) 676-684.

[14] H.J. Walls, S.B. Caines, A.M. Sanchez, S.A. Khan, Yield stress and wall slip phenomena in colloidal silica gels, Journal of Rheology (1978-present) 47(4) (2003) 847-868.

[15] J.J. Stickel, J.S. Knutsen, M.W. Liberatore, W. Luu, D.W. Bousfield, D.J. Klingenberg, C.T. Scott, T.W. Root, M.R. Ehrhardt, T.O. Monz, Rheology measurements of a biomass slurry: an inter-laboratory study, Rheologica Acta 48(9) (2009) 1005-1015.

[16] T.C. Nguyen, D. Anne-Archard, V. Coma, X. Cameleyre, E. Lombard, C. Binet, A. Nouhen, K.A. To, L. Fillaudeau, In situ rheometry of concentrated cellulose fibre suspensions and relationships with enzymatic hydrolysis, Bioresource Technology 133 (2013) 563-572.

[17] Y. Sun, J. Cheng, Hydrolysis of lignocellulosic materials for ethanol production: a review, Bioresource Technology 83(1) (2002) 1-11.

[18] F. Carvalheiro, L.C. Duarte, F.M. Gírio, Hemicellulose biorefineries: a review on biomass pretreatments, Journal of Scientific & Industrial Research 67 (2008) 849–864.

606 [19] G. Pierre, Z. Maache-Rezzoug, F. Sannier, S.A. Rezzoug, T. Maugard, High-
607 performance hydrolysis of wheat straw using cellulase and thermomechanical
608 pretreatment, Process Biochemistry 46(11) (2011) 2194-2200.
609 [20] W.E. Kaar, M.T. Holtzapple, Benefits from Tween during enzymic hydrolysis of
610 corn stover, Biotechnology and Bioengineering 59(4) (1998) 419-427.
611 [21] C. Roche, C. Dibble, J. Knutsen, J. Stickel, M. Liberatore, Particle concentration
612 and yield stress of biomass slurries during enzymatic hydrolysis at high-solids loadings,
613 Biotechnol Bioeng 104 (2009) 290 - 300.
614 [22] L. Rosgaard, P. Andric, K. Dam-Johansen, S. Pedersen, A.S. Meyer, Effects of
615 substrate loading on enzymatic hydrolysis and viscosity of pretreated barley straw,
616 Applied Biochemistry and Biotechnology 143(1) (2007) 27-40.
617 [23] M. Vázquez, M. Oliva, S.J. Téllez-Luis, J.A. Ramírez, Hydrolysis of sorghum
618 straw using phosphoric acid: Evaluation of furfural production, Bioresource Technology
619 98(16) (2007) 3053-3060.
620 [24] M. Chang, T.C. Chou, G. Tsao, Structure, pretreatment and hydrolysis of cellulose,
621 Bioenergy, Springer Berlin Heidelberg1981, pp. 15-42.
622 [25] R. Dasari, K. Dunaway, R. Berson, A scraped surface bioreactor for enzymatic
623 saccharification of pretreated corn stover slurries, Energy Fuel 23 (2009) 492 - 497.
624 [26] C.C. Geddes, J.J. Peterson, M.T. Mullinnix, S.A. Svoronos, K.T. Shanmugam,
625 L.O. Ingram, Optimizing cellulase usage for improved mixing and rheological
626 properties of acid-pretreated sugarcane bagasse, Bioresource Technology 101(23)
627 (2010) 9128-9136.
628 [27] L.T.C. Pereira, L.T.C. Pereira, R.S.S. Teixeira, E.P.D. Bon, S.P. Freitas, Sugarcane
629 bagasse enzymatic hydrolysis: rheological data as criteria for impeller selection, Journal
630 Of Industrial Microbiology & Biotechnology 38(8) (2011) 901-907.
631 [28] B.-H. Um, Optimization of Ethanol Production from Concentrated Substrate,
632 Auburn University, 2007, p. 268.
633 [29] J. Du, F.Z. Zhang, Y.Y. Li, H.M. Zhang, J.R. Liang, H.B. Zheng, H. Huang,
634 Enzymatic liquefaction and saccharification of pretreated corn stover at high-solids
635 concentrations in a horizontal rotating bioreactor, Bioprocess. Biosyst. Eng. 37(2)
636 (2014) 173-181.
637 [30] N.V. Pimenova, A.R. Hanley, Effect of corn stover concentration on rheological
638 characteristics, Applied Biochemistry and Biotechnology 113 (2004) 347-360.
639 [31] B. Frémaux, Eléments de cinétique et de catalyse, Lavoisier, Paris, 1989.
640 [32] L. Michaelis, M.L. Menten, Die Kinetik der Invertinwirkung, Biochem 49 (1913)
641 333-369.
642 [33] J. Chrastil, Enzymatic product formation curves with the normal or diffusion
643 limited reaction mechanism and in the presence of substrate receptors, Int. J. Biochem.
644 20(7) (1988) 683-693.
645
646

Figure 1: Experimental methodology and strategy

Figure 2: Configuration of bioreactor and impellers (dimensions in mm)

Figure 3: Overview of in-situ and ex-situ rheometry. A: In-situ viscometry as a function of hydrolysis time. B: Viscous, G" (open symbols), and elastic, G' (filled symbols), as a function of shear stress (3%-0.5 signifies 3% dm and 0.5 mL enzyme/g cellulose).

Figure 4: Yield stress during hydrolysis versus dry matter content (1%-0.5 stands for: 1% dm and 0.5 mL enzyme/g cellulose)

Figure 5: Uniqueness of dimensionless viscosity-time curves (1%-0.5 signifies 1% dm and 0.5 mL enzyme/g cellulose).

Figure 6: Overview of in-situ (FBRM) particle size analysis: A: Chord number and B: Mean chord.

Figure 7: Population balance (classes defined from initial chord length distribution), in-situ viscosity, and hydrolysis yield during hydrolysis (1%-0.5 mL enzyme/g cellulose case).

Figure 8: Reduction of physico-biochemical parameters during hydrolysis using kinetic models (for 3% w/v, 0.5 mL enzyme/g cellulose)

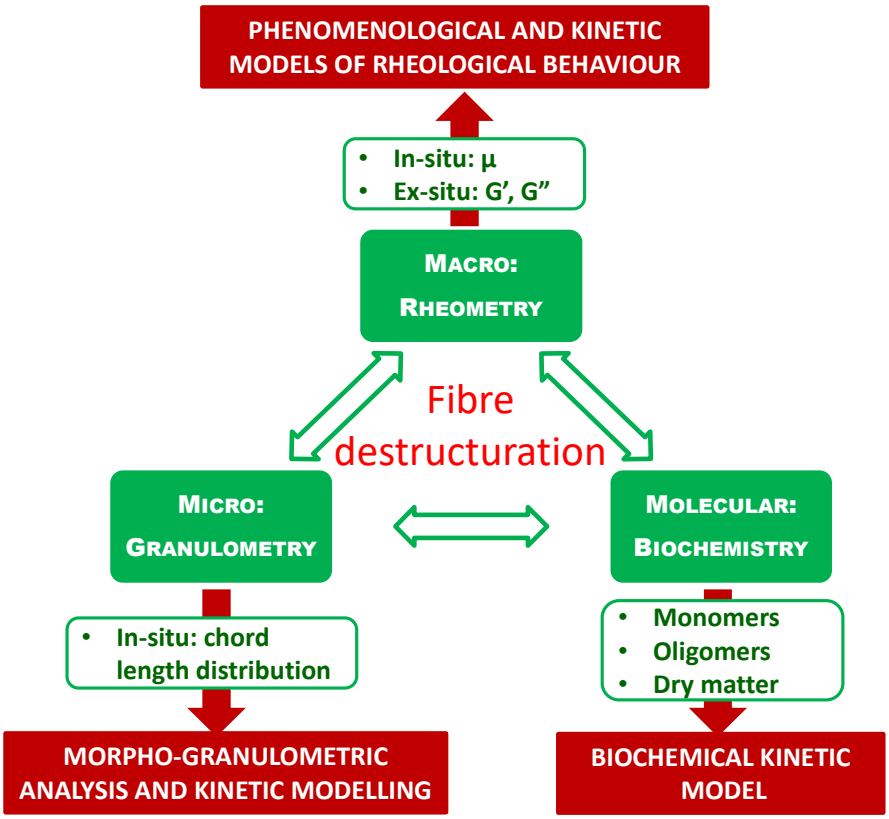
PHENOMENOLOGICAL AND KINETIC MODELS OF RHEOLOGICAL BEHAVIOUR
• In-situ: μ
• Ex-situ: G', G"
MACRO: RHEOMETRY
Fibre destructuration
MICRO: GRANULOMETRY
MOLECULAR: BIOCHEMISTRY
• In-situ: chord length distribution
• Monomers
• Oligomers
• Dry matter
MORPHO-GRANULOMETRIC ANALYSIS AND KINETIC MODELLING
BIOCHEMICAL KINETIC MODEL

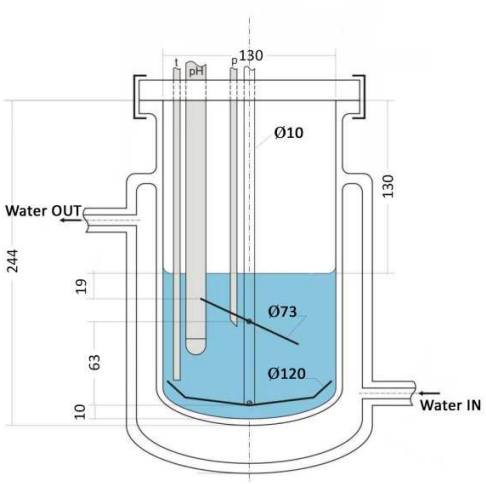

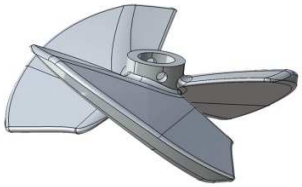

Agitator ϕ73
Height: 38

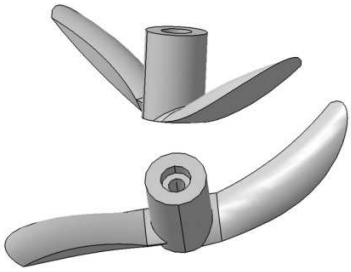

Agitator ϕ120
Height: 22

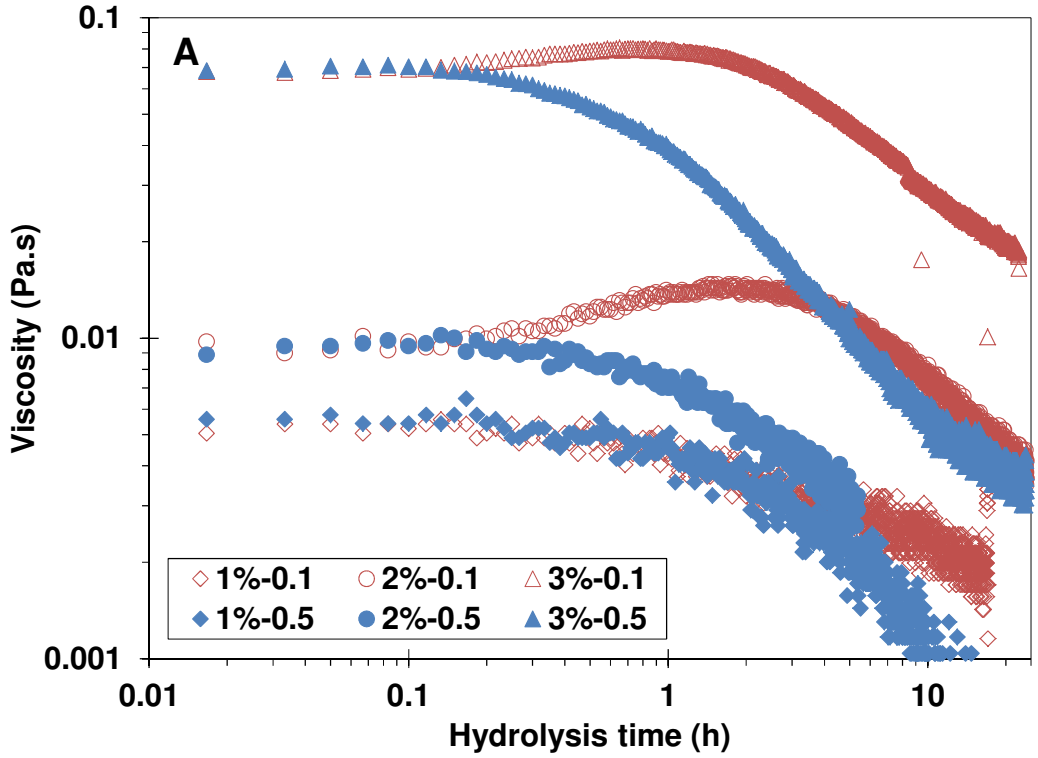
A
Viscosity (Pa.s)
0.1
0.01
0.001
0.01
0.1
1
10
Hydrolysis time (h)
1%-0.1
2%-0.1
3%-0.1
1%-0.5
2%-0.5
3%-0.5

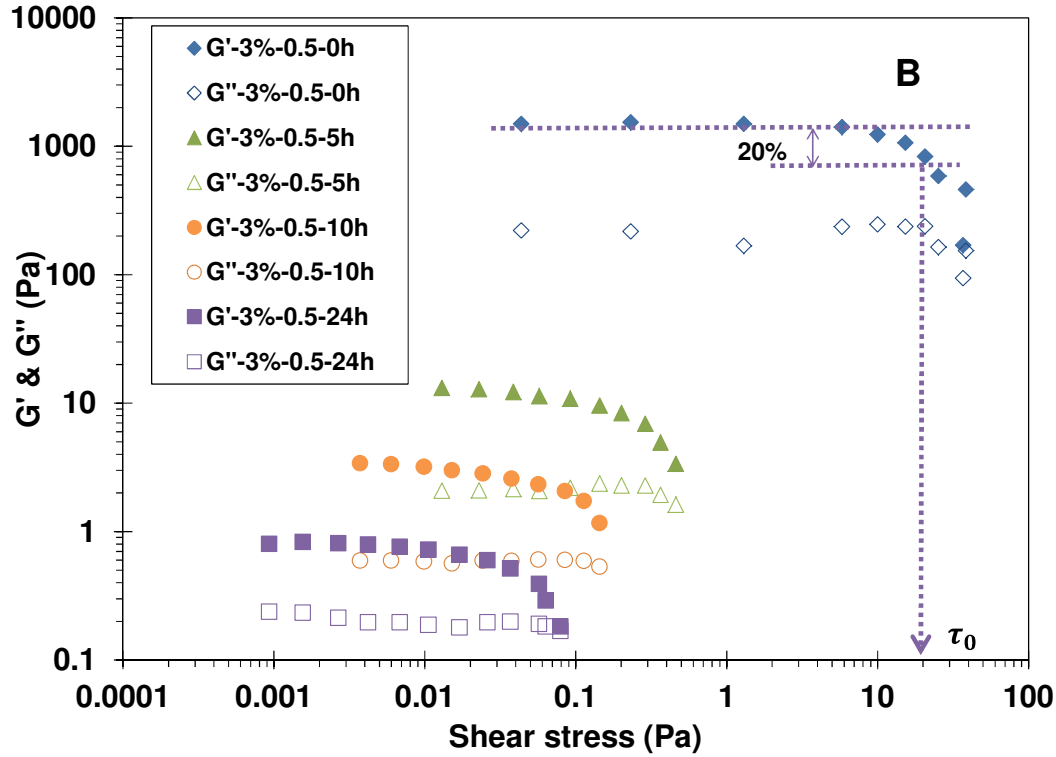
B
G' & G'' (Pa)
10000
1000
100
10
1
0.1
0.0001
0.001
0.01
0.1
1
10
100
Shear stress (Pa)
G'-3%-0.5-0h
G''-3%-0.5-0h
G'-3%-0.5-5h
G''-3%-0.5-5h
G'-3%-0.5-10h
G''-3%-0.5-10h
G'-3%-0.5-24h
G''-3%-0.5-24h
20%
τ_0

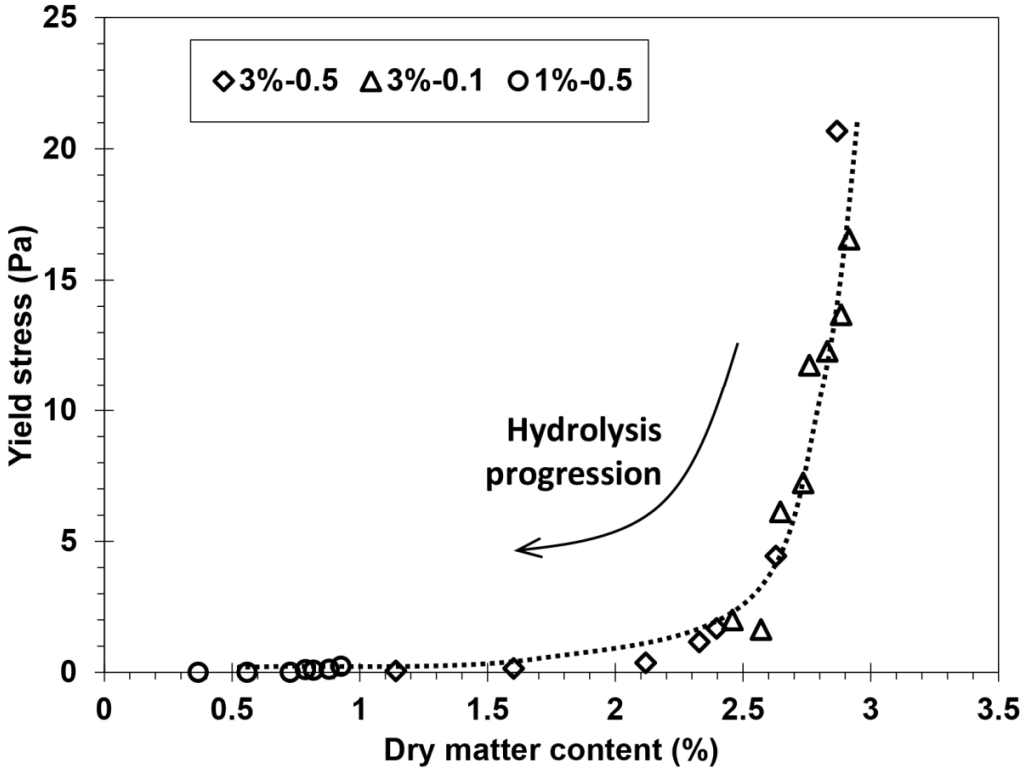
3%-0.5
3%-0.1
1%-0.5
Hydrolysis progression
Yield stress (Pa)
Dry matter content (%)
0
5
10
15
20
25
0
0.5
1
1.5
2
2.5
3
3.5

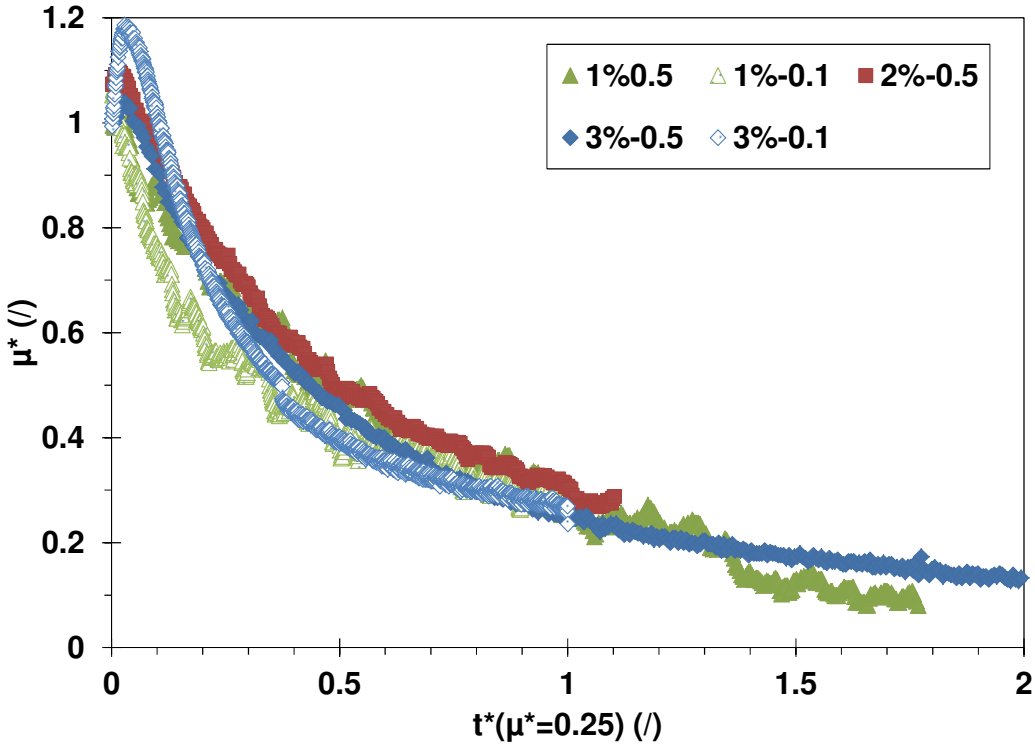
1.2
1
0.8
0.6
0.4
0.2
0
μ* (/)
0
0.5
1
1.5
2
t*(μ*=0.25) (/)
1%0.5
1%-0.1
2%-0.5
3%-0.5
3%-0.1

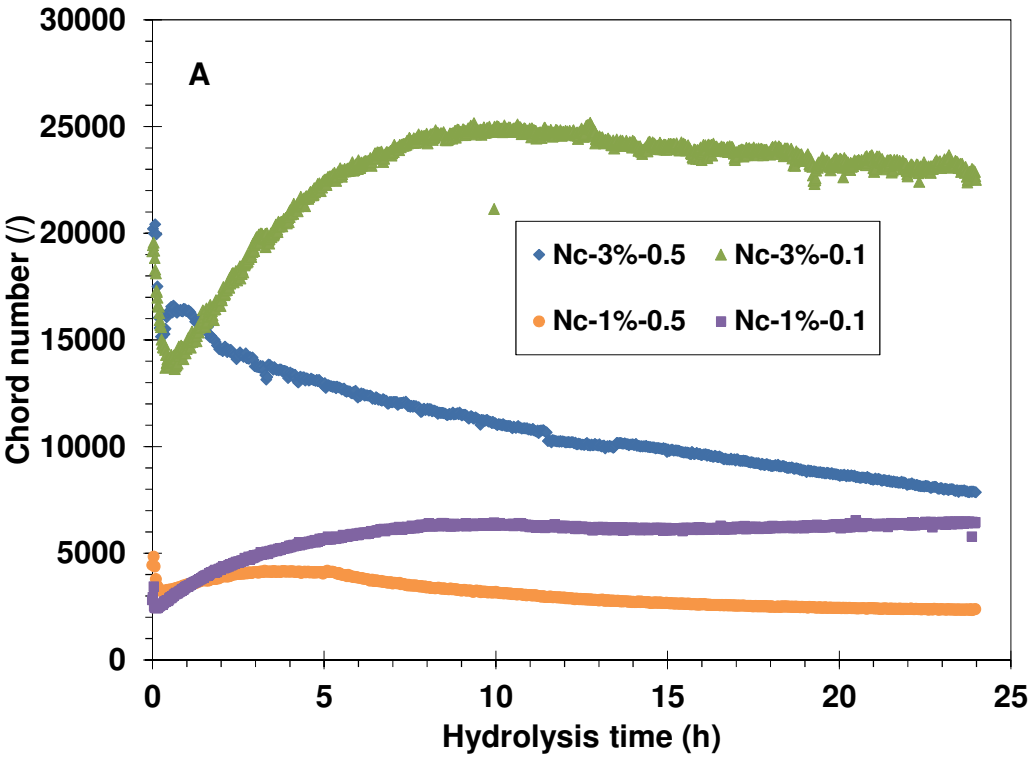
A
Chord number (/)
30000
25000
20000
15000
10000
5000
0
0
5
10
15
20
25
Hydrolysis time (h)
Nc-3%-0.5
Nc-3%-0.1
Nc-1%-0.5
Nc-1%-0.1

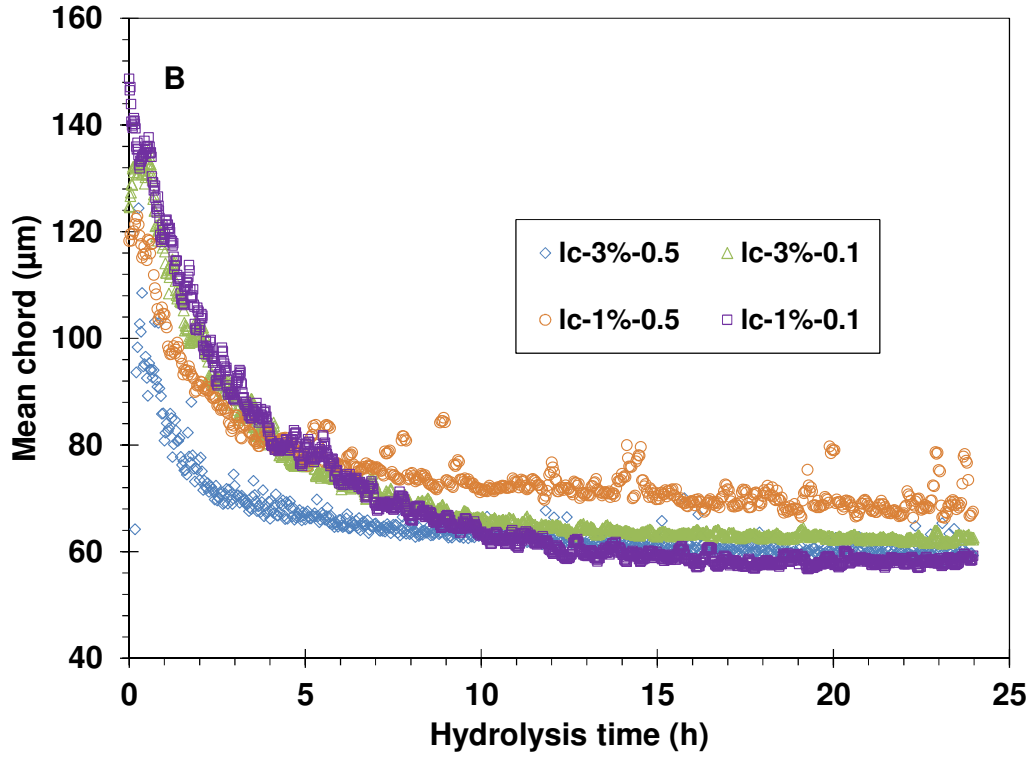
B
Mean chord (µm)
160
140
120
100
80
60
40
0
5
10
15
20
25
Hydrolysis time (h)
lc-3%-0.5
lc-3%-0.1
lc-1%-0.5
lc-1%-0.1

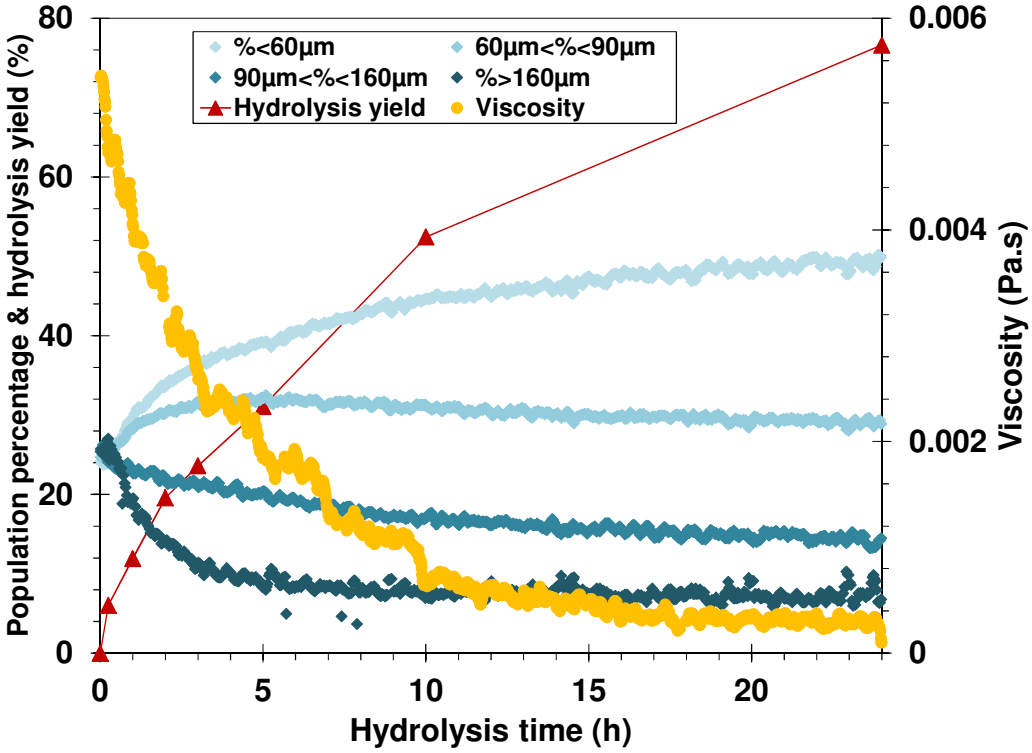
%<60µm
60µm<%<90µm
90µm<%<160µm
%>160µm
Hydrolysis yield
Viscosity
Population percentage & hydrolysis yield (%)
Viscosity (Pa.s)
Hydrolysis time (h)
0
20
40
60
80
0
0.002
0.004
0.006
0
5
10
15
20

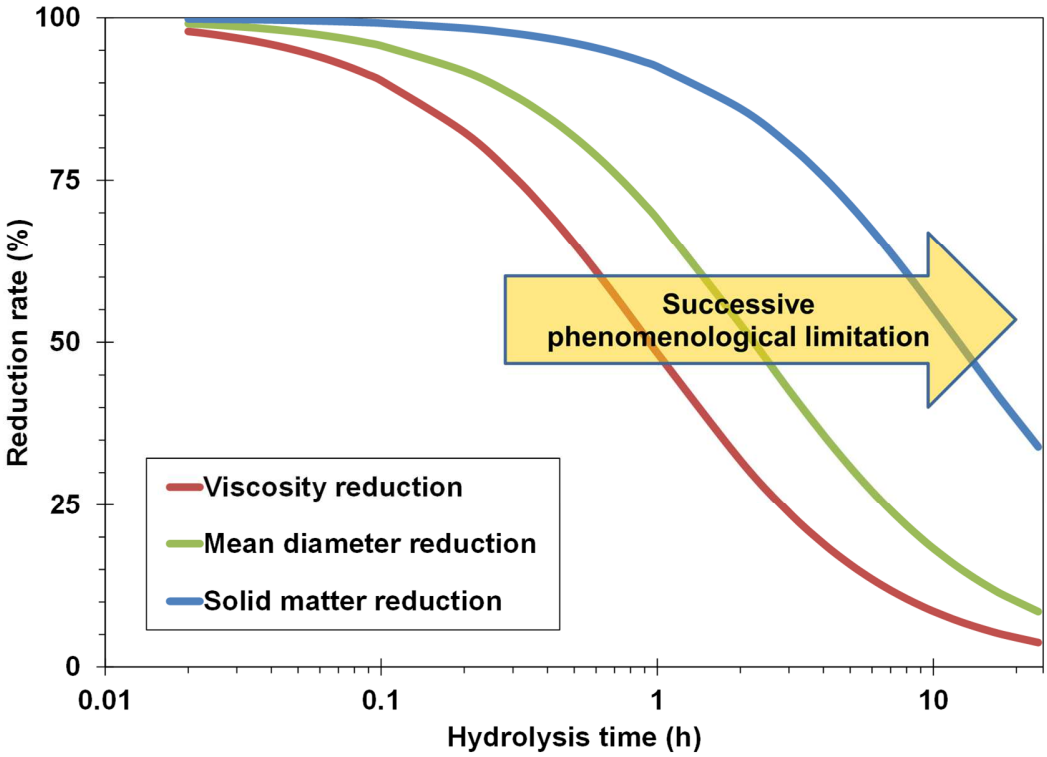
100
75
50
25
0
Reduction rate (%)
0.01
0.1
1
10
Hydrolysis time (h)
Successive
phenomenological limitation
Viscosity reduction
Mean diameter reduction
Solid matter reduction

Table 1: Bioconversion rate (%) during enzyme hydrolysis

Substrate concentration (%gdm.L^{-1})	Enzyme/Substrate (mL/g cellulose)	0h	0.25h	2h	5h	10h	24h	Mass balance (24h,%)
1	0.1	0	1.0	4.7	9.6	11.6	13.2	93.7
1	0.5	0	6.0	19.6	31.1	52.4	76.6	94.1
3	0.1	0	1.3	6.4	11.3	14.5	19.1	94.6
3	0.5	0	6.0	20.6	32.7	54.1	73.5	95.2

Table 2: Kinetic coefficients of rheological, granulometric ($lc_{m\infty}$ in µm) and biochemical parameters, and associated correlation coefficients R^2.

Coefficient	1%w/v		3%w/v	
	0.1mL/g cellulose	0.5mL/g cellulose	0.1mL/g cellulose	0.5mL/g cellulose
k_μ ($Pa^{-1}.s^{-2}$)	-	61.5	2.1	15.3
R^2	-	0.936	0.979	0.988
k_{lc} ($\mu m^{-1}.s^{-1}$)	$8.1x10^{-3}$ (65 µm)	$44.7x10^{-3}$ (66 µm)	$9.0x10^{-3}$ (60 µm)	$32.1x10^{-3}$ (59 µm)
R^2	0.875	0.876	0.950	0.938
k_S ($(gdm/L)^{-1}.s^{-1}$)	$7.6x10^{-3}$	$71.7x10^{-3}$	$3.7x10^{-3}$	$26.9x10^{-3}$
R^2	0.822	0.987	0.885	0.995